

FABRICATION OF TUNGSTEN FIBER ARRAYS IN GLASS AND
ELECTROCHEMICAL ETCHING OF TUNGSTEN WIRE

by

Daniel A. Schaeffer

A senior thesis submitted to the faculty of

Brigham Young University - Idaho

in partial fulfillment of the requirements for the degree of

Bachelor of Science

Department of Physics

Brigham Young University - Idaho

December 2008

Copyright © 2008 Daniel A. Schaeffer

All Rights Reserved

BRIGHAM YOUNG UNIVERSITY - IDHAO

DEPARTMENT APPROVAL

of a senior thesis submitted by

Daniel A. Schaeffer

This thesis has been reviewed by the research committee, senior thesis coordinator, and department chair and has been found to be satisfactory.

Date

Evan Hansen, Advisor

Date

David Oliphant, Senior Thesis Coordinator

Date

Stephen Turcotte, Committee Member

Date

Stephen Turcotte, Chair

ABSTRACT

FABRICATION OF TUNGSTEN FIBER ARRAYS IN GLASS AND ELECTROCHEMICAL ETCHING OF TUNGSTEN WIRE

Daniel A. Schaeffer

Department of Physics

Bachelor of Science

Due to its high melting point and other excellent material properties, tungsten has become a material of choice for field emission cathodes. We have developed a scalable technique to rapidly produce tungsten field emitter arrays. Using a modified fiber drawing process, micron sized tungsten wire is coated with a thin layer of glass and cut into fibers. The glass coated fibers are fused together to create an array of uniaxially aligned wires embedded in glass. Wafers are then cut from the glass fusion and etched in hydrofluoric acid to expose the ends of the tungsten wires. Electrochemical etching is used to sharpen the tips to a radius of curvature that is less than 200nm. Hydrofluoric acid is used to further etch away the glass and expose the tungsten tips. Field emission studies were then carried out to characterize the performance of the individual tips in the tungsten cathode array.

ACKNOWLEDGMENTS

I would like to thank my internship mentors John Simpson and Brian D'Urso for providing me with a wonderful opportunity to be part of this research and also the rest of the research group at Oak Ridge National Laboratory. Many thanks to the BYU-Idaho Physics Department Faculty for their support and a special thanks to Evan Hansen, my research advisor, Stephen Turcotte, and David Oliphant for helping me through the writing process. I would also like to thank the Department of Energy for funding my internship and allowing my internship to be possible.

Contents

Table of Contents	xi
List of Figures	xiii
1 Introduction	1
2 Fabrication of Arrays	5
2.1 Literature Review	5
2.2 Glass Properties	8
2.2.1 Soda-lime Glasses	10
2.2.2 Borosilicate Glasses	12
2.3 Tungsten Properties	16
2.4 Fabrication Sequence	17
2.4.1 Drawing	18
2.4.2 Fusion	22
2.4.3 Slicing and Polishing	23
2.5 Glass Etching	24
3 Electrochemical etching	27
3.1 Literature Review	27
3.2 Etching Process	28
3.2.1 Setup	28
3.2.2 Procedure	29
3.3 Results of Etch	30
4 Field Emission	33
4.1 Literature Review	33
4.2 Application	36
5 Conclusions	37
Bibliography	38

List of Figures

2.1	Advantek Draw Tower schematic	20
3.1	Schematic of electrochemical etching setup	28
3.2	Sequence for fabrication of tungsten wire array embedded in glass . .	31
4.1	Sommerfeld model for energy distribution of electrons in a metal . . .	34
4.2	Potential configuration for the phenomenon of ‘cold emission’.	35

Chapter 1

Introduction

Macroscopic systems can provide useful tools for analysis and characterization of unknown entities. Understanding the functionality of these systems at microscopic levels can be difficult as behavioral patterns at such scales do not consistently follow macroscopic trends and therefore information at the macroscopic level cannot be interpolated down to the microscopic level. The objective of obtaining functionality at such levels for this thesis can be attributed to various promising factors. One such factor is the amorphous structure of glass which provides homogeneous properties at incredible variation in sizes and forms. Another factor is the relevance of significant properties such as diffusion and local electrical behavior compared to macroscopic systems.

The research carried out for this thesis involved developing an ordered structure of tungsten wire arrays in a glass matrix using a fiber drawing technique. Many past techniques for fabricating composite arrays have involved complex and expensive procedures. Fiber drawing, by comparison, is a reproducible, effective method for developing such arrays. These wire array tips were then prepared for low voltage field emission using an electrochemical etching process utilizing the standard "drop-off"

technique [1].

The motivation for this thesis has its foundation based off the principle of fiber optic drawing. Earlier research similar to this thesis, done with different composites of glass [2] [3], has recently been performed with much success. The thought is then, if it is possible to draw nano-featured fibers with two different glasses, why not two completely different materials. With that initial thought, various materials drawn with glass have been studied. One of the more interesting materials is tungsten, or tungsten wires, with tungsten sealing glasses. As mentioned above, the goal of this thesis was to fabricate an ordered array of tungsten wires embedded in a glass matrix for use as field emission cathodes.

Field emission (FE) is not new to research but all current field emitters consists typically of one wire. Such emitters require high voltages to produce field emission and is also very destructive to the emitters themselves. By creating an array of emitters the goal is to be able to require a lower ‘turn on’ voltage allowing the electrons from the emitter to overcome the potential barrier much easier. Such an idea opens the way to many different and useful potential applications.

A few applications include tips for scanning electron microscopes (SEM), tunneling electron microscopes (TEM), and scanning tunneling microscopes (STM) which require low voltages and therefore less power and energy consumption. Another area that this idea may be applied to is lighting. By having a conducting wire in a glass (an insulating material), directionally conducting fibers may be produced on the microscale and can replace conventional lighting we now use. Once again, requiring very low voltages to produce field emission, the fibers may be used in conjunction with a gas to excite the electrons which in turn eventually emit photons to produce cheaper, more efficient lighting. One last example of a potential application is the use in displays. By creating a large array of the tungsten wires, the emitted electrons may be

accelerated to an electron sensitive screen where an image is displayed. Producing these arrays on the nanoscale provide a cheaper, more efficient display than an LCD or LED display.

Chapter 2

Fabrication of Arrays

2.1 Literature Review

Nanostructured systems have in the recent decades generated considerable interest in both basic and applied research as well as in commercial applications. Glass fiber arrays as a confined system is of unique interest because of their extraordinary optical and electrical properties. The topic of this thesis for generating tungsten wire arrays using a fiber drawing fabrication technique was inspired by the work on arrays of nanocone glass [3]. The idea of drawing, bundling, and fusing dissimilar glasses, however, is based on the work of arrays of nanochannel glass [4], which mainly differs from nanocone glass in the reversal of the core and cladding glasses.

A successful fiber draw occurs when a preform — several pieces of a glass with differing electrical and optical properties, to provide the core and cladding of the fiber to be manufactured — placed in an oven is heated and reaches an optimal viscosity. For standard glass/glass draws and when drawing glass with a refractory metal (such as tungsten) the optimal viscosity is typically somewhere around $10^{7.6}$ dPa·s. This glass temperature viscosity, η , is considered the softening point and is achieved at

approximately 825 °C for standard borosilicate glasses. The normal range of viscosity for a glass draw is between about 10^5 to 10^8 dPa·s. In this region of temperatures the glass flow rate can be optimized and subsequently controlled quite readily, which shall be shown by varying the draw speed.

The dynamics of fiber drawing obey simple laws of physics. Conservation of volume is observed and therefore the volume of glass entering the draw furnace per unit time must equal the volume of glass fabricated. Simply stated, the amount of material that goes in must come out. Mathematically speaking, the product of the preform's cross-sectional area and feed rate (rate at which glass is introduced into the furnace) must equal the resultant fiber cross-sectional area and draw rate (rate at which glass is pulled). This can be expressed as

$$D \times (\text{Fiber Cross-sectional Area}) = F \times (\text{Preform Cross-sectional Area})$$

where D and F are the draw and feed rates, respectively, in meters per minute (MPM). By solving for the draw rate, one can calculate the required speed to obtain a given fiber diameter. For round preforms it follows that

$$D = F \times \frac{(\text{O.D.}_{clad}^2 - \text{I.D.}_{clad}^2) + \text{O.D.}_{core}^2}{\text{O.D.}_{fiber}^2} \quad (2.1)$$

where O.D. is outside diameter (mm) and I.D. is inside diameter (mm).

The following example, adapted from the 'Fiber Optic Straight-Draw Tower' [5], will illustrate how to calculate the draw speed control parameter and how the effects of speed variation control fiber size (diameter):

Some typical preform and fiber dimensions for cladding glass tubing are O.D. = 34.5mm and I.D. = 32.5mm and a core rod with dimensions O.D. = 31.0mm which will manufacture the desired fiber with O.D. = 0.50 mm.

It follows then from equation 2.1 that the draw rate equals

$$D = F \times \left(\frac{(34.5 \text{ mm})^2 - (32.5 \text{ mm})^2 + (31 \text{ mm})^2}{(.5 \text{ mm})^2} \right)$$

$$D = F \times (4380)$$

Using this relationship and selecting a feed rate F of .0065 MPM (a typical value) we obtain the draw rate

$$D = (.0065 \text{ MPM}) \times (4380) = 28.47 \text{ MPM}$$

To appreciate the effect of Draw Speed variation on fiber size control we will examine the mathematical partial $\delta\emptyset/\delta v$ where \emptyset represents the width of the fiber diameter. The easiest way to demonstrate this relationship is by calculating the draw speed for a 0.501mm rod ($\Delta\emptyset=0.001\text{mm}$) and a 0.510mm rod ($\Delta\emptyset=0.01\text{mm}$) using the preform dimensions and feed speed of the previous calculation to find the difference (i.e. $\Delta\emptyset/\Delta v$).

Calculation 1 ($\emptyset = 0.501\text{mm}$):

$$D = F \times \frac{(34.5 \text{ mm})^2 - (32.5 \text{ mm})^2 + (31 \text{ mm})^2}{(.501 \text{ mm})^2}$$

$$D = F \times (4362.5)$$

Using this relationship for a feed rate of .0065 MPM:

$$D = (0.0065 \text{ MPM}) \times (4362.5) = 28.36 \text{ MPM}$$

$$\Delta v = 28.47 \text{ MPM} - 28.36 \text{ MPM} = 0.11 \text{ MPM}$$

$$\Delta\emptyset/\Delta v = 0.001 \text{ mm}/0.11 \text{ MPM} = 9.10 \mu\text{m}/\text{MPM}$$

Calculation 2 ($\emptyset = 0.510\text{mm}$):

$$D = F \times \frac{(34.5 \text{ mm})^2 - (32.5 \text{ mm})^2 + (31 \text{ mm})^2}{(.510 \text{ mm})^2}$$

$$D = F \times (4209.9)$$

Using this relationship for a feed rate of .0065 MPM:

$$D = (0.0065 \text{ MPM}) \times (4209.9) = 27.36 \text{ MPM}$$

$$\Delta v = 28.47 \text{ MPM} - 27.36 \text{ MPM} = 1.11 \text{ MPM}$$

$$\Delta\emptyset/\Delta v = 0.010 \text{ mm}/1.11 \text{ MPM} = 9.00 \mu\text{m}/\text{MPM}$$

It can be seen that under these conditions substantial draw speed changes must take place (greater than 1.0 MPM) to affect the diameter by 0.010mm. By further inspection we can see that a typical line speed variation of ± 0.01 MPM only affects the diameter by ± 0.0001 mm.

2.2 Glass Properties

Glass is an inert material that is widely used throughout the world and is compatible with many other elements. It is a relatively inexpensive and a common material that can be obtained easily and in bulk quantities. By definition [6], glass is defined as an amorphous solid completely lacking in long-range periodic atomic structure and exhibiting a region of glass transformation behavior. It is formed by cooling a liquid, which is at a temperature well above the melting temperature of that substance, down to a temperature below its melting temperature without crystallization.

It has been found that drawing two different glasses — a cladding and a core — with high contrasting etch rates but similar linear thermal expansion coefficients is possible [3] and can produce a variety of results. Commercially available glasses can be divided into a few major categories. The following are the most common produced and used for a wide variety of applications. These are the glasses that were considered to be used for drawing with tungsten wire.

1. Vitreous silica is the least compositionally complex commercial glass available and is primarily used for optical fibers, ultraviolet and infrared transmitting optics, and for applications requiring high temperatures. Vitreous silica is the only commercial glass which contains only a single major chemical component and is often produced from the naturally occurring mineral quartz. Although a wonderful glass by itself, due to its high glass transformation temperature and slightly incompatible thermal expansion coefficient, vitreous silica is not a good match with other glasses or with tungsten and therefore was not used to make the fiber array.
2. Soda-lime-silica glasses are the most prevalent type of glass, used for windowpanes, glass containers (bottles and jars) for beverages, food, and some commodity items. Soda-lime glass is typically divided into glass used for windows—called float glass or flat glass—and glass for containers—called container glass. Both types differ in the application, production method (float process for windows, blowing and pressing for containers), and chemical composition.
3. Borosilicate glasses refractory properties and physical strength make it ideal for use in laboratories, where it is used to make high-durability glass lab equipment, such as beakers and test tubes. In addition, due to its low thermal expansion coefficient, borosilicate glass warps minimally when exposed to heat allowing a borosilicate container to provide accurate measurements of volume over time.

The most important properties of commercial glasses are the density, refractive index, thermal expansion coefficient, glass transformation temperature, and chemical durability. These properties for specific chemical compositions of the glasses used in the fabrication process will be shown in the next section.

2.2.1 Soda-lime Glasses

Soda-lime silica glasses are by far the most produced type of glass by weight. Soda-lime glass compositions represent a compromise between many of the outstanding properties of pure silica and cost efficiency. By adding soda, lime, and other raw materials the transformation temperature greatly decreases providing a low-melt glass, ideal for situations where high temperatures need to be avoided. The composite of soda, lime, and silica also increase the durability of the glass itself and becomes very ductile, while on the other hand the chemical durability of the glass decreases drastically along with an increase in the thermal expansion coefficient becoming more susceptible to thermal shock.

The density and refractive index of soda-lime glasses are greater than vitreous silica, which can be related to chemical durability [7]. Another important change that occurs is the electrical conductivity of the glass. The electrical conductivity of most oxide glasses results from diffusion of monovalent ions under the influence of an applied electric field [6] and addition of soda sharply reduces the electrical resistivity of the glass. This is an undesired result as we want the glass to be as insulating as possible to avoid any interference between the tungsten fibers embedded in the glass matrix.

AR-Glas®

AR-Glas® is a clear glass of the third hydrolytic class and a soda lime glass type with a high content of alkali and alkaline earth oxides. It has a much higher thermal expansion coefficient and therefore cannot be drawn with Schott 8330 Duran® or Schott 8487 (see section 2.2.2). It does have high transmission ($\geq 90\%$) for wavelengths as short as 350 nm to 2500 nm and is ideally used for pharmaceutical applications but is also common for lighting, laboratory equipment, and electronics.

Because of its high thermal expansion coefficient, AR-Glas® is not the ideal glass to be used with tungsten, but can be done. Special precautions must be taken to ensure that the glass forms a nice coating of the tungsten wire and that the wire does not break while drawing. AR-Glas® does have a very low transformation temperature, though, and it has been found that it is useful when using other refractory metals with higher thermal expansion coefficients or other materials such as carbon nanotubes.

Below is a table listing the properties of AR-Glas® and their respective values. The values for chemical resistance are listed in classes where a lower number represents a higher resistance.

Table 2.1 Properties of Commercially Available AR-Glas® Soda-lime Glass

Physical Data	Property	Value	Units
	Mean thermal expansion coefficient	9.1	10^{-6}K^{-1}
	Transformation temperature T_g	525	$^{\circ}\text{C}$
	Glass temperature viscosity η		dPa·s
	10^{13} (annealing point)	530	$^{\circ}\text{C}$
	$10^{7.6}$ (softening point)	720	$^{\circ}\text{C}$
	10^4 (working point)	1040	$^{\circ}\text{C}$
	Dielectric constant ϵ	7.2	
	Refractive index n_d ($\lambda = 587.6\text{nm}$)	1.514	
Chemical Resistance	Property	Class	
	Hydrolytic resistance	HGB 3	
	Acid resistance	S1	

2.2.2 Borosilicate Glasses

The use of a borosilicate glass is desirable because of its high chemical and thermal resistance. It is available in a wide variety of compositions and thence has a wide variety of properties, of which may be tinkered with to be able to obtain desired results. In general, borosilicate glasses have a much greater resistance to thermal shock and higher electrical resistivity. Listed below is a small selection of different types of borosilicate glasses that have characteristics matching the criteria to draw with tungsten wire.

Schott 8330 Glass

Schott 8330 (Duran®) is matched well with Schott's 8487 glass since they have similar coefficients of expansion and contrast each other very well in their chemical properties. In addition to the high compatibility with 8487, Schott's 8330 glass was chosen because it is produced in such massive quantities and therefore can be quite easily purchased. Table 2.2 lists the values of some important properties for 8330.

Schott 8337B Glass

8337B is a highly specific borosilicate glass and is very expensive. It is used mainly in applications that require UV transmitting glass. This type of glass is also a tungsten sealing glass and for that reason there was an interest in using it. Its thermal expansion coefficient is very close to tungsten and makes a nice seal around the tungsten fibers when drawn together. As can be seen by comparing table 2.3 and 2.4, it is nearly equivalent to the 8487 glass in its contrast to etchability with Duran®; however, due to its high cost and relatively low drawing temperatures, 8337B was not used to make the tungsten fiber arrays.

Table 2.2 Properties of Commercially Available Duran® (Pyrex) Glass

	Property	Value	Units
Physical Data	Mean thermal expansion coefficient	3.3	10^{-6}K^{-1}
	Transformation temperature T_g	525	$^{\circ}\text{C}$
	Glass temperature viscosity η		dPa·s
	10^{13} (annealing point)	560	$^{\circ}\text{C}$
	$10^{7.6}$ (softening point)	825	$^{\circ}\text{C}$
	10^4 (working point)	1260	$^{\circ}\text{C}$
	Dielectric constant ϵ	4.6	
	Refractive index n_d ($\lambda = 587.6\text{nm}$)	1.473	
Chemical Resistance	Property	Class	
	Hydrolytic resistance	HGB 1	
	Acid resistance	S1	

Chemical Composition (approx. wt%): SiO_2 (81%) B_2O_3 (13%) $\text{NaO} + \text{K}_2\text{O}$ (4%) Al_2O_3 (2%)

Table 2.3 Properties of 8337B Borosilicate Glass

	Property	Value	Units
Physical Data	Mean thermal expansion coefficient	4.1	10^{-6}K^{-1}
	Transformation temperature T_g	440	$^{\circ}\text{C}$
	Glass temperature viscosity η		dPa.s
	10^{13} (annealing point)	465	$^{\circ}\text{C}$
	$10^{7.6}$ (softening point)	705	$^{\circ}\text{C}$
	10^4 (working point)	1085	$^{\circ}\text{C}$
	Dielectric constant ϵ	4.7	
	Refractive index n_d ($\lambda = 587.6\text{nm}$)	1.476	
Chemical Resistance	Property	Class	
	Hydrolytic resistance	HGB 3	
	Acid resistance	S4	

Schott 8487 Glass

The 8487 glass combines well with 8330 and many different combinations are able to be produced [3] using these two glasses alone. 8487 glass is not as common as 8330 and typically is not used for general applications, but 8487 is a tungsten sealing glass and creates a near uniform seal (when running a vacuum) around the tungsten wire. 8330 can be used as the cladding for the tungsten fibers and arrays are able to be fabricated but 8487 glass provides a more efficient sealer and results in more controllable, more uniform tungsten fiber arrays. The values for the properties of 8487 are listed in table 2.4 below.

Table 2.4 Properties of 8487 Borosilicate Glass

	Property	Value	Units
Physical Data	Mean thermal expansion coefficient	3.9	10^{-6}K^{-1}
	Transformation temperature T_g	525	$^{\circ}\text{C}$
	Glass temperature viscosity η		dPa·s
	10^{13} (annealing point)	560	$^{\circ}\text{C}$
	$10^{7.6}$ (softening point)	775	$^{\circ}\text{C}$
	10^4 (working point)	1135	$^{\circ}\text{C}$
	Dielectric constant ϵ	4.9	
	Refractive index n_d ($\lambda = 587.6\text{nm}$)	1.479	
Chemical Resistance	Property	Class	
	Hydrolytic resistance	HGB 4	
	Acid resistance	S3	

Chemical Composition (approx. wt%): SiO_2 (75.5%) B_2O_3 (46.5%) $\text{NaO} + \text{K}_2\text{O}$ (1.5%)

Al_2O_3 (4%) CaO (.5%) MgO (.5%)

2.3 Tungsten Properties

Tungsten (W, element 74) is ideal for field emission and high temperature applications because of its robust physical properties. Excluding carbon, tungsten has the highest melting point of all the elements. It is also very durable being extremely chemically resistive and has good conductive properties. Some of tungsten's properties can be itemized [8] as below:

- It is typically brittle and hard to work with, but if pure it can be cut with a hacksaw
- It is worked by forging, drawing, extruding, or sintering.
- Of all metals in pure form, tungsten has the highest melting point (3,422°C)
- It has the lowest vapor pressure and at temperatures above 1,650°C the highest tensile strength.
- It has the lowest coefficient of thermal expansion of any pure metal.

Tungsten has a mean thermal expansion coefficient of $4.5 \cdot 10^{-6} \cdot \text{K}^{-1}$, which compares nicely to the coefficients of 8330 and 8487. This is a necessary compatibility when drawing. If the mean thermal expansion coefficients do not match close enough then too much stress becomes an issue when the glass-tungsten fiber cools.

It is appropriately desired that the thermal expansion coefficient of the glass cladding be slightly less than that of tungsten. This is so because tungsten has a much greater range for which its mean thermal expansion coefficient is valid and will not increase very much with higher temperatures where the values for glass increase more at temperatures close to those needed for drawing, which results in a real value for the thermal expansion coefficient closer to that of tungsten.

2.4 Fabrication Sequence

The first step of fabrication is to determine the method of fabrication. I will briefly explain the methods I used for preparing such samples.

Fiber Drawing. Fiber drawing is most commonly known for making fiber optics.

In the relatively recent years it has extended beyond glass preforms to include materials such as polymers, salts, low-temperature metals, refractory metals, and more. Fiber drawing works by placing a preform into a preform feed at the top of a fiber draw tower. The feed is lowered at a calculated rate into a furnace where the preform melts into a glob and falls by effects of gravity. As the melted preform cools, it is pulled down through a laser micrometer into a tractor system. The now cooled thread is pulled by the tractor belts at a user input feed rate forming a fiber proportional to the original preform.

Fiber drawing is a well know process that is cheap, safe, and provides large quantities of samples per unit time. Fiber drawing also does not require extensive knowledge and expertise to be able to obtain quality results.

Bundling & Fusion. After drawing the necessary fibers the next step is to bundle them together and fuse them so they become one solid rod while maintaining their individual properties. Bundling is quite simple and straightforward. The fibers collected are cleaned and carefully placed in a glass tube (typically of the same material as the cladding) preventing any twisting or cracking. Once enough fibers are in place so as to fill the volume of the tube, this new preform is placed in a vacuum chuck and is ready for fusing.

Since we are interested in the nano-features of the glass/tungsten composite, the goal of the fusion process then is to heat the bundled fibers to a point that

softens the glass and just begins to collapse. This eliminates any gaps and extra spacing between the glass fibers and the glass and tungsten themselves. The result is a continuous, uniform matrix with a fixed alignment of tungsten fibers.

Slicing & Polishing. Once the fusion process is complete the bundle is sliced into wafers and polished. The slicing method must not introduce structural damage and defects to the area under analysis. Slicing is done with a precision saw capable of cutting the glass into wafers as thin as .8mm.

Polishing creates a smooth, shiny, flat, and defect free surface. If the sample is not to be polished by hand then it is wax mounted on a flat metal holder. This is attached to a movable arm in the polisher. The surface to be polished must be kept as parallel as possible to the surface of the polishing area to ensure flatness and uniformity of the finished surface. A water spraying system fed from a reservoir helps keep the sample from overheating due to friction. A series of films (either diamond or silicon carbide) were used to get down to a very fine polished surface. The microstructure of the surface is then examined in an optical microscope to check for a uniformly and evenly polished surface.

2.4.1 Drawing

Nanocone and nanochannel glasses are prepared by combining dissimilar glasses in a core-cladding preform, one of the glasses typically being highly acid etchable. The glass assembly consists of a rod (the core) and a tube (the cladding) suspended vertically above a furnace into which the preform is slowly fed. Other materials may be used to construct the preform to fabricate the application-specific product. The furnace used is based on the type of material being drawn but typical temperature ranges for glass-glass draw is between 600°C–900°C where acceptable ranges for general fiber

drawing is between 150°C–1100°C. After the preform is setup and the desired draw speed entered, the drawing process is fairly straightforward. Using equation 2.1 one can now calculate the required feed speed to produce fibers with the correct diameter.

The Draw Tower

The draw tower used to fabricate the fibers is a custom engineered design from Advantek Engineering. The tower is a modular design and most of the components can be interchanged allowing the draw tower to adapt to the type of drawing required, whether it be low-temperature drawing, polymer drawing, glass drawing, metal drawing, etc.

The tower consists of the following main components: 1) The main structural frame which serves as the support for the rest of the components; 2) A computerized direct drive servo system with custom vacuum chucks to attach to the feed system; 3) A long-life heating oven with a max temperature of 1100°C and compact heating zones for maximum preform yield; 4) A 25kg tractor draw system; 5) A Zumbach laser micrometer; 6) Automatic, adjustable carbide fiber cutter system; 7) A computer touch screen control panel.

A simple schematic of the draw tower (see figure 2.1) shows the operating order of the draw system and is given with the technical data in table 2.5.

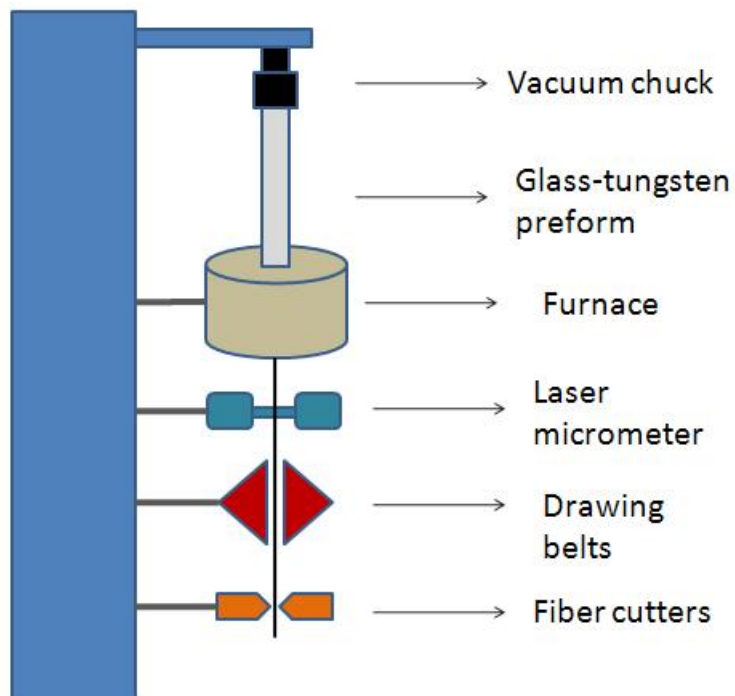
Glass-Glass Draw

For a glass-glass draw the preform is setup in the manner as explained in the previous section. The core glass rod, typically 8330, is placed into a glass tube cladding, typically 8487, with an I.D. similar to the O.D. of the core. The preform is placed in the draw tower and the correct parameters are input into the control panel.

When the temperature reaches the appropriate level the preform is then fed into

Table 2.5 Technical specifications for Advantek Draw Tower

Property	Value
Drawing Speed Range	.5–12 m/min
Feed Speed Range	.0005–1 m/min
Tower Height	3.6 m
Max. Preform Length/Dia.	1000/40 mm
Max./Min. Fiber Dia.	18/.2 mm
Draw Speed Accuracy	$\pm 0.08\%$
Feed Speed Accuracy	± 0.0001 m/min
Max. Oven Temp/Control	1100/.25°C

**Figure 2.1** Advantek Draw Tower schematic

the furnace and the drawing process begins. As the glass fibers come out of the furnace, they cool down by ambient air convection briefly before reaching a pair of rubber belts whose speed directly control the draw rate. Manual draw speed adjustment can stabilize a fluctuating fiber diameter. If the diameter of the fiber increases above its target, the drawing speed is increased; if the fiber diameter starts falling below the target, the drawing speed is decreased. Heating the glass to a sufficient temperature that determines an optimal viscosity is the key to drawing glass.

Glass-Metal Draw

Setup for a glass-metal draw, particularly with tungsten as the metal, was slightly different than for a glass-glass draw in which nanocones or nanochannels are the result. We used an 8487 capillary tube with an inner diameter (I.D.) of roughly 1.1 mm inside an 8487 thin-walled tube of approximately 6 mm outer diameter (O.D.) and a wall thickness of 1 mm. The tungsten wire of diameter $75\mu\text{m}$ was then spooled through the capillary tube.

To calculate the feed speed we first found the effective diameter for the outer cladding for a series of concentric tubes starting with the areas given as

$$(A_{\text{OD}_{\text{clad}}} - A_{\text{ID}_{\text{clad}}}) + A_{\text{OD}_{\text{core}}} = A_{\text{eff}}$$

where A_{OD} refers to the outer diameter area, A_{ID} refers to the inner diameter area, and the difference of the two gives the cladding cross-sectional area, which reduces to

$$\sqrt{d_{\text{OD}_{\text{clad}}}^2 - d_{\text{ID}_{\text{clad}}}^2 + d_{\text{OD}_{\text{core}}}^2} = d_{\text{eff}}$$

where d is the diameter.

For the fiber diameter, the thickness ratio $\frac{\text{OD}}{\text{ID}}$ of the preform will stay constant

as it collapses onto the tungsten wire. We were able to calculate the new O.D. by keeping the ratio the same and the tungsten wire as the new I.D. That is to say

$$\frac{OD_1}{ID_1} = \frac{OD_2}{ID_2}$$

Now we are able to use equation 2.1 to solve for the feed speed required with a given draw speed that we had preselected. By inspecting equation 2.1 we see that our constants divide out and our equation becomes dependent on the diameters.

From this point all that is required is to physically setup up the preform and feed it into the furnace with the parameters set into the draw tower. After enough fibers have been collected they will be bundled together to be fused (section 2.4.2) to form a glass-tungsten rod and annealed to alleviate any stresses. The resultant glass-tungsten rod will then be sliced into thin wafers (section 2.4.3) and then prepared for a series of glass and tungsten etches.

2.4.2 Fusion

The fibers obtained in the draw are collected, sorted to make sure there are no bad fibers (missing tungsten, broken glass, non-uniform cladding, etc), and casually cleaned. To fuse the fibers into a solid rod we bundled the fibers together and methodically placed them into an 8487 tube (approximately 8 mm O.D., 1 mm wall thickness) so that there was minimal twisting of the fibers and stress was evenly distributed.

The fusion preform was then placed into the preform feed on the draw tower and lowered into the furnace so that the entire length of the rod containing the tungsten fibers was within the boundaries of the heating elements of the furnace. We baked the preform at a temperature close to 175°C for approximately one hour to clean any impurities in the fiber bundle. The preform is also placed under a slight vacuum of

10 inHg.

This procedure typically results in a well fused bundle. These parameters have been optimized so that there is minimal bending or curling of the fused rod.

2.4.3 Slicing and Polishing

In order to obtain uniform arrays and tips in the glass and electrochemical etch processes, the fused rod must be sliced into thin wafers and polished. To cut the wafers we used an Isomet 1000 Precision Sectioning diamond cutting saw. It is equipped with a 7" blade and variable speed up to 975 rpm by increments of 25 rpm. The thickness of the wafer is measured using a mechanical lever attached to the sample holder with a digital display. When slicing wafers the blade thickness must be accounted for. Typical sized wafers were on the order of 3 mm in thickness and 5 mm in diameter.

After slicing individual wafers, they were polished using one of three methods which are (1) polishing by hand with metal polishing grids, (2) polishing using diamond polishing grids with a simple automated polisher, and (3) polishing using silicon carbide (SiC) polishing grids on an advanced automated polisher.

Polishing with the first method was a time consuming process and involved manually rubbing the glass wafer on the surface of the metal polishing grid. The setup for this method involved several different polishing grids each with a different grit ranging from 80 (roughest) to 16000 (smoothest). One may progressively move in ascending order (by grit number) from grid to grid polishing the wafer for approximately one minute per grid. One thing to be cautious of when polishing by hand is to be careful not to polish too much, as the wafer can become very thin quickly when polishing on rougher surfaces.

For method two (2) the process can be more or less time consuming than the first method depending on desired smoothness and therefore the advantage for automated

polishing is not a matter of time but of evenness where uniform pressure (i.e. weight of the wafer and mount) is applied with minimal variations in angular velocity. To polish using this method, the sample must be attached to a polishing mount specific to the polisher with mounting wax. The wax is heated up until the sample is able to be set into it and then allowed to cool. The mount is then attached to the polisher. The parameters allowed to be controlled on the simple polisher are the speed, time, distance between sample and diamond grid, and amount of cleaning water allowed to flow onto the sample.

The last method by far has the most control over the process. The sample is placed into a holder specific to the sample size so that mounting wax is not needed (if a sample is made that does not fit any sample holder mounting wax may be used). The sample holder is attached to the polishing arm which is lowered onto the SiC grid. The user is then allowed to choose the amount of polishing time, speed, direction, force applied, and water flow. For the fabrication of tungsten fiber arrays all three methods were utilized with no preference to any one method.

2.5 Glass Etching

Amorphous borosilicate glass is a good candidate for isotropic etching due to its microstructure and diffusion properties. A functional structure on the composite wafer fabricated with the required morphology is obtained by selecting an appropriate etching process. Chemical solution based wet etching and vapor/reactive ion/ sputter based dry etchings are the two common forms of etching. Chemically strong bases and acids may etch glass. Hydrogen fluoride (HF) reacts with the silicates producing soluble silicon fluoride, which diffuses producing a groove. A multicomponent glass etches non-uniformly resulting in a jagged surface. As already seen in the section

on glass properties, glass is easily etched by hydrofluoric acid solution. The etching process is determined by the following parameters [9].

Etching solution. The composition of the fluoride solutions used in the etching of borosilicate glass greatly determines factors in the process chemistry like the etch rate and the surface roughness.

Etching temperature. Temperature can speed up the chemical reaction causing increased etch rate.

Agitation. Ultrasonic stirring continuously exposes the surface of the sample to fresh volumes of acid resulting in enhanced uniformity and etch rate. However the stirring may not be a favorable choice for extremely fine and delicate structure profiles.

After etching, the quality of the etched wafer was determined using SEM microscopy and measured by how well the tungsten wires had been exposed both individually and relative to each other. Also, depending on the glass used, the quality of the etch can be seen by how well the tungsten fibers are set in the glass matrix. Too much etching may cause gaps on the tungsten-glass interface allowing the tungsten wires to become loose.

Chapter 3

Electrochemical etching

3.1 Literature Review

Electrochemical etching of tungsten wire is a subject that has been widely reported on in literature [10] [11] [12]. Tungsten probe tip preparation has been studied thoroughly for scanning tunneling microscopy (STM) and ultra-sharp tips are essential for atomic level techniques. The STM — invented by Binnig and Rohrer [13] in the early 1980's — has become an important instrument in surface science. The STM is based on the idea of quantum tunneling and is highly sensitive to the current between the sample surface and probe tip.

Tungsten may be etched various ways using both wet and dry etch techniques, however, electrochemical methods are ideal for etching of tungsten and common electrolytes used are KOH and NaOH [10], which have been used extensively in related research and applications. The basic principle of electrochemical etching is to take the array of tungsten wire and immerse it in the electrolyte which is placed in a beaker surrounded by a conducting ring so that the tips of the tungsten wire are the anode and the ring is the cathode. The electrochemical reaction during tip prepara-

tion involves anodic dissolution of tungsten in aqueous medium [10]. A potential is then applied between the two electrodes and the electrochemical etching takes place where the actual etching occurs at the electrolyte/air interface.

3.2 Etching Process

After the fabrication of the glass wafers containing the tungsten wire array, the samples will be prepared for two types of etching — glass etching, as discussed in section 2.5, and tungsten etching. Upon obtaining a desirable glass-etched sample exposing the tungsten fibers, the tips embedded in the glass matrix are sharpened using an electrochemical process. By setting up a simple circuit (figure 3.1), one may provide an experiment that allows important data such as electrolyte type and concentration, etch time, voltage, etc. to be collected and later analyzed.

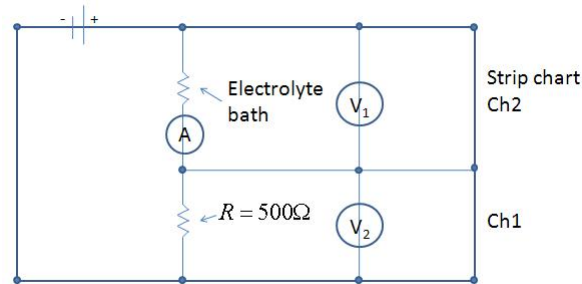


Figure 3.1 Schematic of electrochemical etching setup

3.2.1 Setup

The experimental setup used for the tungsten etch consists of a wire wound precision resistor, a glass beaker containing the electrolyte, a circular platinum ring shaped to fit the lining of the glass beaker placed in the solution, and the tungsten wire array mounted to a brass cylinder which in turn is attached to a micro-positioner. The

brass cylinder, cut specifically to fit the sample to be etched, was hollowed out at the tip and then lined with indium foil. The sample was then placed into the brass cylinder with the indium foil providing electrical contact and extra holding strength. The wire is positioned into the solution making the electrical circuit complete.

With later etches it was discovered that not every wire was included in the circuit and some of the tips were not being etched. By sputter coating a thin layer of gold across the backside of the sample, contact is made with every wire and a more uniform etch results.

3.2.2 Procedure

A sample from one of our fusions (see section 2.4.2) was used to sharpen the tungsten wire tips. The etching was done using the electrochemical process described above. We used 2 M NaOH as our electrolyte and a platinum wire ring was our cathode leaving the tungsten wire as the anode. We applied a potential of 5 V across the electrolyte bath and a 500 Ω wire wound precision resistor which was in series with the electrolyte. The resistor is included to be able to control the current through the electrolyte.

We monitored the voltage and current using a chart recorder. During an etch, the chart recorder shows a steady decrease in current and increase in potential. The drop-off of the tips occurs when there is a sudden change in the current and increase in potential. For our first etch experiment our potential was applied for approximately 1.5 hours but was learned that 20–25 min is sufficient for a sample of approximately 5mm in diameter.

3.3 Results of Etch

The quality of the resulting etched wafer can be measured by a few parameters. One such parameter is the structure accuracy, that is, whether the structure shows under-etched blunted cones or over-etched tips that appear to be elongated and have difficulty remaining standing vertically. This structure accuracy is important both for individual wires and for the array as a whole.

Another feature that is very important that can be explored using an SEM is tip sharpness. This is one of the more desirable and important parameters to control, as the main focus of this thesis is to be able to obtain nano-tips in tungsten arrays consistently within the array itself and repeatedly. This can be mostly controlled by tuning the amount of time allowed for the tips to remain in the electrolyte solution and in some cases the etchant itself. A few images showing the results of some of the etching experiments performed are shown on the following page.

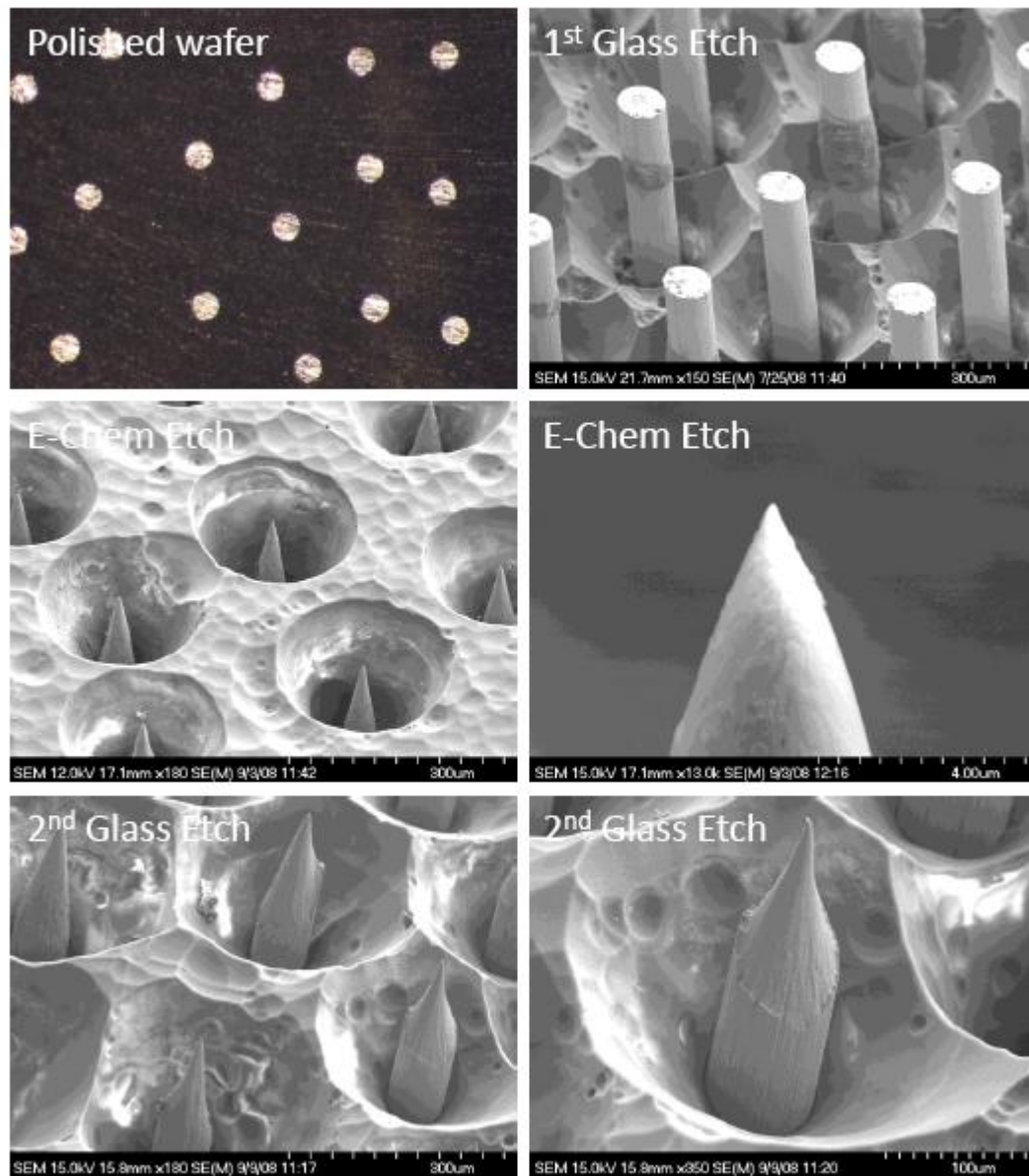


Figure 3.2 Sequence for fabrication of tungsten wire array embedded in glass

Chapter 4

Field Emission

4.1 Literature Review

The field emission (FE) of electrons from a cold metallic cathode in the presence of a large surface electrical field was first reported by Robert H. Wood (1899). Field emission is different than thermionic emission, a phenomenon where electrons only with sufficient kinetic energy above the potential barrier escape into the surrounding phase.

At frequency ν , the energy of a photon is $h\nu$. When striking the metal surface, the photon interacts with an electron and ejects it from the metal. Consider the *Sommerfeld model* [14] of a conducting metal shown in figure 4.1. The conductor is composed of fixed positive sites and free electrons

The energy of the highest filled level in the metal is called the Fermi energy E_F , and is equal to the chemical potential of electrons in the metal. The energy difference between the Fermi level and the potential energy of electrons is the thermionic work function [15] ϕ . In the absence of an external field, the potential barrier becomes infinite and the electrons must obtain enough energy to overcome this barrier, as in

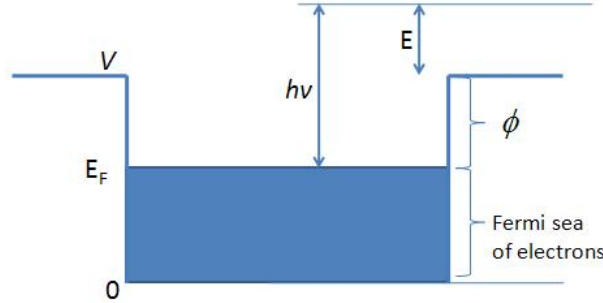


Figure 4.1 Sommerfeld model for energy distribution of electrons in a metal

the case of thermionic emission. With an external field present the potential barrier is modified and at distances at or near the surface the potential barrier is finite so that tunneling may occur provided the barrier is thin enough.

The Fowler-Nordheim theory is generally used to quantitatively describe FE which requires using the FE current density j as a function of the electric field. Since this process is a tunneling process, the tunneling transition probability for the electron to tunnel through the potential barrier and the number of electrons incident on the potential barrier must be found. The probability P of barrier penetration can be expressed by the Wentzel-Kramer-Brillouin (WKB) method as

$$P = \text{Const} \times \exp \left[-2^{\frac{3}{2}} m^{\frac{1}{2}} / \hbar \int_0^l (V - E)^{\frac{1}{2}} dx \right] \quad (4.1)$$

where m is the mass of the particle, \hbar is Plank's constant divided by 2π , E and V are the kinetic and potential energy, respectively, and l is the width of the barrier. Since the area under the curve $(V - E)^{1/2}$ is approximately triangular [15], it may be expressed as

$$\int_0^l (V - E)^{\frac{1}{2}} dx \approx \frac{1}{2} \phi^{\frac{1}{2}} \times \phi / F \approx \frac{1}{2} \phi^{\frac{3}{2}} / F \quad (4.2)$$

where F is the field strength. Substituting equation (4.2) into (4.1), the probability

P for the electrons near the Fermi energy level becomes

$$P = \text{const} \times \exp \left[(2^{\frac{1}{2}} m^{\frac{1}{2}} / \hbar) \phi^{\frac{3}{2}} / F \right] \quad (4.3)$$

By taking the product of the number electrons arriving at the surface with the tunneling probability the current density is given as

$$j = \frac{4\sqrt{\mu\phi}}{\mu + \phi} \frac{e^3 F^2}{8\pi\hbar\phi} \exp \left[-\frac{8\pi\sqrt{2m}\phi^{\frac{3}{2}}}{3\hbar e F} \right] \quad (4.4)$$

where μ is the Fermi level relative to the bottom of the conduction band.

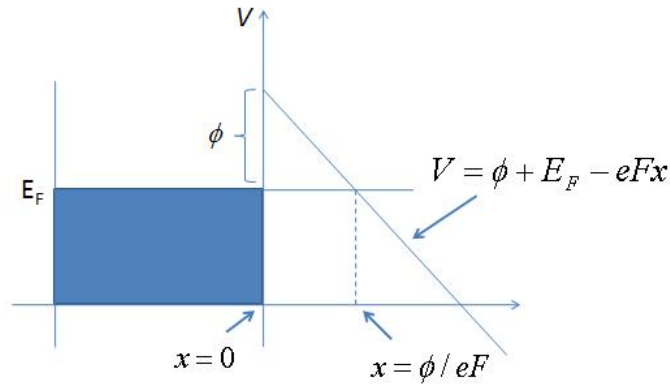


Figure 4.2 Potential configuration for the phenomenon of ‘cold emission’.

From equation (4.4) it can be seen that the current increases with the square of the voltage (expressed in the electric field F), multiplied by an exponential constant proportional to the inverse of the electric field. The electric field is where the focus of my research turns. In the phenomenon of field emission, also known as *cold emission*, electrons are drawn from a metal (near room temperature) by an externally supported electric field. The potential well that the metal presents to the free electrons before the electric field is turned on is depicted in figure 4.1. After application of the constant electric field, F , the potential at the surface slopes down as shown in figure 4.2, thereby allowing the electrons in the Fermi sea to tunnel through the potential barrier.

By providing tips with small radii of curvature the electric field near the tip becomes large and the energy (of the electrons) per unit area increases. Literature suggests that it is possible to draw various combinations of materials as long as the mean linear thermal expansion coefficients are approximately equivalent. It has also been shown that single fiber tungsten wire can be etched to tips $\leq 5\text{nm}$ in radius of curvature [16]. By combining these two methods it is possible to draw tungsten wire within a glass matrix, place them in an array, and produce sharp tips capable of field emission.

4.2 Application

The field emission microscope (FEM) is one of the primary applications of the field emission phenomena. The introduction of commercial FEMs enabled more accurate field calculations, which confirmed the validity of the Fowler-Nordheim theory within experimental error.

In addition to the applications of FE to surface science studies, FE is used in vacuum microelectronic devices, which rely on electron transport through vacuum rather than carrier transport in semiconductors. Displays based on field emitter arrays are by far the most common use of vacuum microelectronic devices. These field emission displays generally replace the thermal cathodes of traditional cathode ray tube displays with arrays of field emitters. In addition to applications in display technology, several other vacuum microelectronic devices have been demonstrated, including FE triodes and amplifiers and microwave frequency devices

Chapter 5

Conclusions

This thesis has discussed the method of fabricating micron-sized tungsten wires for field emission in a unique, modified fiber drawing process, coating them with a glass cladding. Tungsten was chosen for various reasons but most importantly for its high melting point. By fusing the glass-coated fibers an array of uniaxially aligned wires is produced. Wafers are then cut from the glass fusion and electrochemical etching proceeds, sharpening the tips to a radius of curvature approximately 100nm. Field emission testing can now be done on the arrays and characterization of the wire arrays may be performed to determine the quality of the tips as field emitters and how they compare to single tip emitters.

My research presents a project with which much may be learned and expand current knowledge of fiber drawing techniques along with STM tip preparation. Despite the copious amount of work previously done there is still much to research and explore. Fiber drawing is a deep well of opportunity where new frontiers are constantly being explored. The work I have done can also provide information to various fields of science and builds upon past accomplishments and successes.

One such area where future research can lead is carbon nanotubes [17]. By replac-

ing the tungsten wire with carbon nanotubes the applications expand even more. A very unique and interesting idea could be creating nano capacitors capable of storing coulombs of charge. By placing these in appropriate circuits, they have the possibility of replacing batteries and could provide a very useful power supply.

The beauty of this project lies in its ability to help in the understanding of many core physics ideas, at the foundation of science, while providing practical and useful information that may be applied to everyday life.

Bibliography

- [1] Liu Anwei, Hu Xiaotang, Liu Wenhui, and Ji Guijun. An improved control technique for the electrochemical fabrication of scanning tunneling microscopy microtips. *Rev. Sci. Instrum.*, 68(10):3811–3813, 1997.
- [2] B. D’Urso, J. T. Simpson, and M. Kalyanaraman. Emergence of superhydrophobic behavior on vertically aligned nanocone arrays. *App. Phys. Lett.*, 90(4), 2007.
- [3] B. D’Urso, J. T. Simpson, and M. Kalyanaraman. Nanocone array glass. *J. Micromech. Microeng.*, 17(4):717, 2007.
- [4] R. J. Tonucci, B. L. Justus, A. J. Campillo, and C. E. Ford. Nanochannel array glass. *Science*, 258(5083):783–785, 1992.
- [5] Advantek Engineering Inc., 7575 Kingspoint Parkway, Suite 6, Orlando, FL 32819. *Fiber Optic Straight-Draw Tower*, 2005.
- [6] J. E. Shelby. *Introduction to Glass Science and Technology*. The Royal Society of Chemistry, 2 edition, 2005.
- [7] Z. Teixeira, O. L. Alves, and I. O. Mazali. *J. Amer. Ceram. Soc.*, 90(1):256–263, 2007.
- [8] A. Stwertka. *A Guide to the Elements*. New York: Oxford University Press, 2 edition, 2002.

-
- [9] Meena Kalyanaraman. Fabrication and a study of the wetting properties of nanostructures surfaces. Master's thesis, The University of Tennessee, Knoxville, 2007.
- [10] A. I. Oliva, A. Romero G., J. L. Peña, E. Anguiano, and M. Aguilar. Electrochemical preparation of tungsten tips for a scanning tunneling microscope. *Rev. Sci. Instrum.*, 67(5):1917–1921, 1996.
- [11] J. K. Cochran, A. T. Chapman, D. N. Hill, and K. J. Lee. Low-voltage field emission from tungsten fiber arrays in a stabilized zirconia matrix. *J. Mater. Res.*, 2(3):322–328, 1987.
- [12] K. S. Yeong and J. T. L. Thong. Life cycle of a tungsten cold field emitter. *Journal of Applied Physics*, 99(10):104903, 2006.
- [13] G. Binnig and H. Rohrer. *IBM J. Res. Develop.*, 30(355), 1986.
- [14] R. L. Liboff. *Introductory Quantum Mechanics*. Addison Wesley, 4 edition, 2003.
- [15] D. P. Woodruff and T. A. Delchar. *Modern Techniques of surface science*. Cambridge University Press, 1992.
- [16] O.L. Guise, J.W. Ahner, M.-C. Jung, P.C. Goughnour, and J.T. Yates. Reproducible electrochemical etching of tungsten probe tips. *Nano Lett.*, 2(3):191–193, 2002.
- [17] L. R. Baylor, V. I. Merkulov, E. D. Ellis, M. A. Guillorn, D. H. Lowndes, A. V. Melechko, M. L. Simpson, and J. H. Whealton. Field emission from isolated individual vertically aligned carbon nanocones. *J. Applied Physics*, 91(7):4602–4606, 2002.